Nanoscale Res Lett (2006) 1:74–78
DOI 10.1007/s11671-006-9003-y

NANO EXPRESS

Guided self-assembly of lateral InAs/GaAs quantum-dot molecules for single molecule spectroscopy

L. Wang · A. Rastelli · S. Kiravittaya · R. Songmuang · O. G. Schmidt · B. Krause · T. H. Metzger

Published online: 26 July 2006

Abstract We report on the growth and characterization of lateral InAs/GaAs (001) quantum-dot molecules (QDMs) suitable for single QDM optical spectroscopy. The QDMs, forming by depositing InAs on GaAs surfaces with self-assembled nanoholes, are aligned along the [$1\bar{1}0$] direction. The relative number of isolated single quantum dots (QDs) is substantially reduced by performing the growth on GaAs surfaces containing stepped mounds. Surface morphology and X-ray measurements suggest that the strain produced by InGaAs-filled nanoholes superimposed to the strain relaxation at the step edges are responsible for the improved QDM properties. QDMs are Ga-richer compared to single QDs, consistent with strain-enhanced intermixing. The high optical quality of single QDMs is probed by micro-photoluminescence spectroscopy in samples with QDM densities lower than 10^8 cm^{-2}.

Keywords Lateral quantum-dot molecules · Quantum dots · Quantum dot composition · Self-assembled growth

Semiconductor quantum dots (QDs) have attracted extensive attention in recent years mostly motivated by the perspective of using them as a medium for storage and manipulation of quantum bits (qubits) [1]. To realize operations between qubits, coupled QD systems are essential [2]. The simplest case consists of a quantum-dot molecule (QDM) composed of two interacting QDs. A well-developed technique to fabricate QDMs with high structural and optical quality is based on the epitaxial growth of vertically stacked self-assembled QDs [3–6]. Two coupling mechanisms can be distinguished, i.e., electron and/or hole tunneling [3, 4, 6] or electromagnetic coupling, typically dipole–dipole interaction of excitons [5, 7]. Since the QDs composing a QDM are usually different, the tuning into resonance is often achieved by using an external tuning parameter such as an electric field [4, 6]. Ideally, also the barrier between the QDs composing a QDM should be tuned independently. This may be achieved by positioning a gate electrode between the two QDs. While such a task is technologically challenging for the vertical geometry, it may be easier for a lateral geometry as suggested previously [8]. Since self-assembled QDs are typically characterized by a flat geometry, the nature of the lateral coupling may differ appreciably from that of vertical coupling, rendering the study of laterally coupled QDs of fundamental interest.

The growth of laterally coupled QDs is mostly based on the random occurrence of spatially close QDs [9]. Recently, we have invented a fabrication technique allowing the controlled growth of lateral QDMs [8, 10–12]. The method is based on the growth of InAs on a GaAs surface decorated with nanoholes. With a proper choice of growth parameters, QDMs aligned in the [$1\bar{1}0$] direction are obtained. A complete understanding of the QDM formation process is still missing. Moreover, since the QDMs are self-assembled, a certain number of isolated QDs is still observed in such samples.

L. Wang · A. Rastelli (✉) · S. Kiravittaya · R. Songmuang · O. G. Schmidt
Max-Planck-Institut für Festkörperforschung, Heisenbergstrasse 1, D-70569 Stuttgart, Germany
e-mail: A.Rastelli@fkf.mpg.de

B. Krause · T. H. Metzger
European Synchrotron Radiation Facility, Boîte Postale 220, F-38043 Grenoble Cedex, France

Here, we succeed in reducing the number of isolated QDs by growth of InAs on a slightly rough GaAs (001) surface. By combining atomic force microscopy (AFM), X-ray diffraction (XRD) and anomalous scattering experiments, we gather a deeper insight into the QDM formation process and we propose a simple explanation for the observed improvement of the QDM homogeneity. By means of a ''guided'' self-assembly of QDMs we increase the relative number of QDMs, and we are able to reduce the QDM surface density down to values lower than 1 μm^{-2}. Such properties render the QDMs an ideal playground to study the properties of single QDMs by means of standard micro-photoluminescence (μ-PL) spectroscopy and coherent optics experiments. From X-ray data we find that the investigated QDMs have higher Ga concentration than single QDs due to strain-enhanced intermixing of In and Ga. This observation is supported by the relative larger size of QDMs due to reduced strain and a slightly blue-shifted emission of QDMs compared to single QDs [8].

The explored structures are grown on GaAs (001) substrates by solid source molecular beam epitaxy combined with atomic-layer-precise $AsBr_3$ in situ etching [8, 11, 13]. After a 200 nm GaAs buffer, we grow InAs QDs by deposition of 1.8 monolayers (ML) InAs followed by 20 nm GaAs, 20 nm $Al_{0.4}Ga_{0.6}As$ and 20 nm GaAs at a substrate temperature of 500 °C. Because of the reduced surface diffusivity of GaAs at this temperature, the surface of the cap layer shows stepped mounds, which are used to guide the nucleation of InAs QDs and QDMs as described below. InAs QDs are grown on this surface followed by a 10-nm GaAs cap and a nominal 5-nm deep $AsBr_3$ etching, resulting in the formation of nanoholes [8, 10, 11]. The nanoholes are overgrown with InAs with varying thickness to investigate the QDM formation process. For optical investigations we grow low density QDMs. In this case the In flux is stopped as soon as a spotty reflection high-energy electron diffraction pattern appears [14]. The emission of the QDMs is blue-shifted by partially capping them with 2 nm GaAs followed by 4 min annealing at 500 °C. (For details on the partial capping and annealing procedure, see ref. [15]) 100 nm GaAs, 20 nm $Al_{0.4}Ga_{0.6}As$ and 20 nm GaAs complete the structure. AFM in tapping mode is employed to characterize the surface morphology of the samples. In XRD measurements, the (220) and (2$\bar{2}$0) diffraction patterns are recorded at an incident angle of 0.15° with an X-ray energy of 10.3 keV. Anomalous X-ray scattering is used to determine the composition of QDMs. Optical investigations are performed by means of the μ-PL setup described in ref. [16]. The μ-PL spectra are collected at a temperature of 6 K either with an InGaAs array detector or with a Si-CCD camera. The spatial and spectral resolution of the used setup are about 2 μm and 80 μeV, respectively.

The InAs QDs grown on a rough surface, which is produced by overgrowth of InAs QDs, have a average height of about 12.8 nm and a surface density of 3 ×

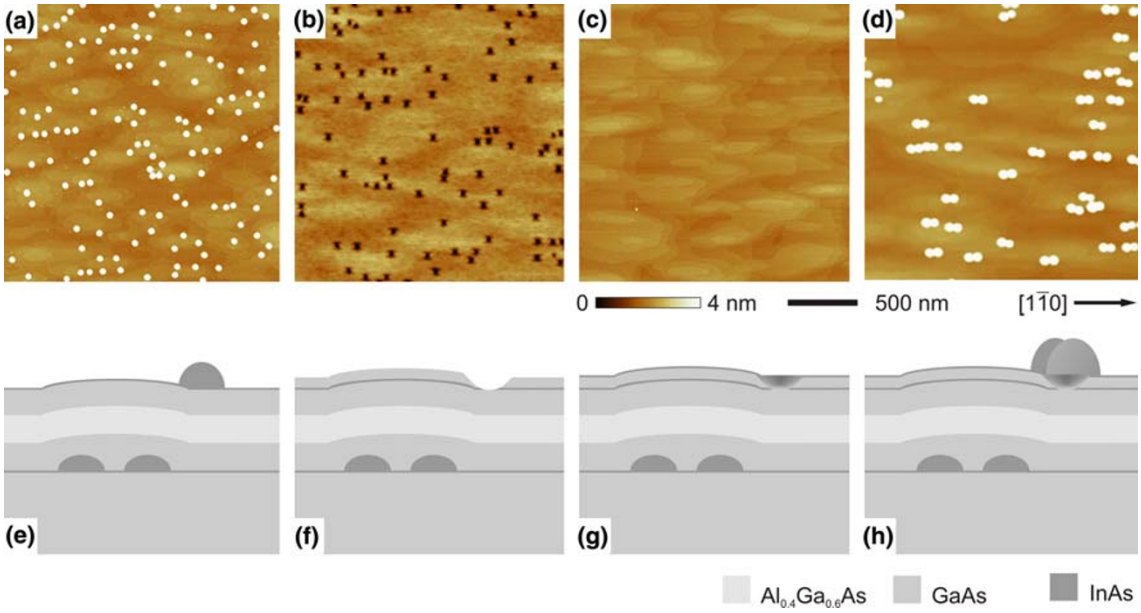

Fig. 1 AFM images of InAs QDs grown on a GaAs surface with stepped mounds generated by a buried InAs QD layer (**a**), GaAs nanoholes (**b**), GaAs nanoholes overgrown with 1 ML of InAs (**c**) and QDMs formed by deposition of 2.5 ML of InAs on nanoholes (**d**). Figures (**e**)–(**h**) represent corresponding schematics of the sample structures in the [110] direction

10^9 cm^{-2} as shown in Fig. 1a. Stepped mounds composed of several MLs of GaAs, elongated in the [1$\bar{1}$0] direction due to the anisotropic growth of GaAs, can be identified in the same figure. We observed that all the QDs nucleate at the convex edges of the mounds [17, 18]. This behavior is attributed to the maximum strain relaxation at these sites [17]. Once the QDs are overgrown by GaAs followed by in situ selective etching, bow-tie-shaped nanoholes elongated in the [110] direction form at the positions previously occupied by the QDs (Fig. 1b). Although the selective etching produces a roughness at the atomic scale, the mounds can be still distinguished. When the nanoholes shown in Fig. 1b are overgrown with 1 ML of InAs, the surface becomes atomically flat and the stepped mounds with well-defined atomic steps reappear (see Fig. 1c). As reported in ref. 8, a filling-up of the nanoholes with InGaAs precedes the QDM formation. Surprisingly, no trace of the nanoholes, nor of the forming QDMs is seen for 1 ML InAs coverage. In order to exclude that the nanoholes fill up during the cooling process preceding the AFM measurement, we have also grown a control sample in which 1 ML AlAs (with very low surface diffusion coefficient) was deposited on top of 1 ML InAs to ''freeze'' the surface before cooling. Also in this case no residual trace of the nanoholes is observed. Nevertheless, lateral QDMs aligned in the [1$\bar{1}$0] direction form at the convex sides of the stepped mounds when further InAs is supplied (see Fig. 1d). The average height of InAs QDMs is about 17.6 nm, which is larger than that of single QDs. The QDM yield, defined as the ratio of number of QDMs divided by total number of QDMs and isolated QDs is improved from about 60% [8] to about 90% by ''guiding'' the self-assembled growth by means of stepped mounds.

To confirm the presence of filled-up nanoholes in the sample shown in Fig. 1c and to gather deeper insight in the QDM formation process, we have performed radial and angular XRD measurements on two samples, one with nanoholes and the other with nanoholes overgrown with 1 ML of InAs. The radial scans of the (220) and (2$\bar{2}$0) reflections are displayed in Fig. 2a, b. For both samples, the radial measurements show well-defined Bragg peaks and oscillations, while the peak shape in angular direction is a Lorentzian. This shows that the scattering contrast is mainly related to the strain within the sample. The (220) reflections are narrower than the (2$\bar{2}$0) reflections, indicating that the strain field of the nanoholes has an elongated shape in the [110] direction which is maintained after the filling. This result is consistent with the hole shape observed by AFM. The less symmetric (2$\bar{2}$0) reflections

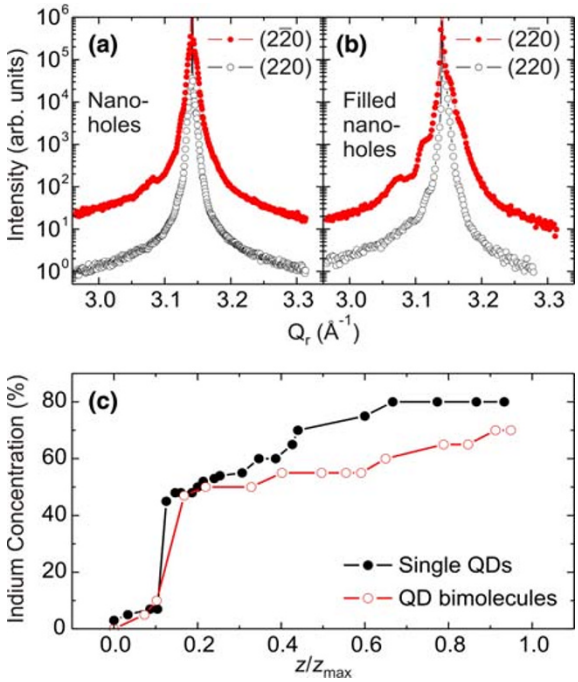

Fig. 2 Radial scans of the (220) and (2$\bar{2}$0) peaks of the GaAs nanoholes (**a**) and nanoholes filled with 1 ML InAs (**b**) and In concentration of QDs and QDMs as a function of normalized height (**c**)

show more pronounced oscillations in both samples. However, the oscillations in the sample with empty nanoholes (Fig. 2a) are much less pronounced than those in the sample with filled nanoholes (Fig. 2b). In the former sample, the small oscillations indicate the existence of residual strain stemming from small amounts of remaining unetched InGaAs in the [1$\bar{1}$0] direction, possibly due to the elongation of the overgrown InAs QDs in this direction [8]. After filling of the nanoholes, the InGaAs mixture in the holes produces additional strain, which results in the more pronounced oscillations (Fig. 2b). For the filled holes, the oscillations in the (2$\bar{2}$0) reflection are more evident than in the (220) peak, implying that the strain is anisotropic and is prominent in the [1$\bar{1}$0] direction. The asymmetric strain field of different filled holes must be very similar, since otherwise the oscillations would be washed out.

The local strain generated by InGaAs-filled nanoholes affects the composition of the formed QDMs. This is demonstrated by anomalous X-ray scattering performed on two samples, one with single QDs and the other with QDMs. The scattering intensity of InGaAs is directly related to the X-ray energy and the Ga concentration. From radial measurements of QDs performed at several energies close to the Ga absorption edge, the vertical In concentration profile within

the QDs can be determined directly from the experimental data, with the concentration as the only free parameter. The results are plotted in Fig. 2c as a function of QD height z, normalized to the maximum QD height z_{max}. The values of In concentrations at normalized heights between 0 and 0.12 are dominated by the strain field in the substrate and should not be considered as reliable values. For larger heights, the In concentration is found to be smaller in the QDMs than in the single QDs. This result is consistent with the observed larger size of the QDs composing the QDMs and the slightly blue-shifted emission of QDMs compared to single QDs. A qualitative explanation for this observation is that strain produces an enhanced diffusivity of Ga, thus enhancing In–Ga intermixing in the forming QDMs. A similar behavior has been widely observed for growth of vertically stacked QDs [19, 20].

Since the deposition of InAs on the nanoholes at 500 °C produces a flat surface prior to the QDM formation (Fig. 1c), we believe that the formation mechanism of QDMs differs substantially from the QDM formation at lower temperatures (450–470 °C). In the latter case, the surface curvature plays a significant role in the formation process since the nanoholes are not completely filled before the QDM formation [8]. Relaxation of strain at the rim of incompletely filled holes is responsible for the QDM formation. In case of the growth on nanohole surface at higher temperature (500 °C), we propose an alternative scenario of the QDM formation as follows: First, during the hole filling process, the deposited In atoms will directionally diffuse toward the bottom of the holes since the surface of convex curvature provides a lower chemical potential at these positions. In addition, during the diffusion at this high temperature, In atoms will substantially intermix with Ga atoms on the surface to increase the entropy of intermixing [21]. Due to the variation of curvature as well as the intermixing, the nanoholes are filled with InGaAs with inhomogeneous In profile inside the holes. The higher In content is expected at the central region of the filled holes (Fig. 3a). Later, when we further deposit In atoms on flat, filled-hole surface, the InAs thickness will reach the critical thickness and the QDs will form. The QDs will form earlier at the filled-hole regions since In atoms prefer to diffuse to these areas due to the lowering of strain energy compared to the QD nucleation on flat surface without filled holes. The nucleation of In adatoms can occur prior to the diffusion to the center since there is a slow-down of the In hopping rate when they are approaching the lower strain region [22]. Consequently, the QDs will form at the region around the center on the filled holes. In addition to this slow-down mechanism, these QDs might preferentially form into QDMs aligned along the $[1\bar{1}0]$ direction due to the influence of the strain relaxation at the step edges (Fig. 3a). Consequently, we conclude that the alignment of the steps and the additional strain relaxation enhance the slow-down mechanism, which produces higher yield of QDMs aligned in the $[1\bar{1}0]$ direction. The schematic of the QDMs formation on filled holes is shown in Fig. 3b. We note here that the buried InAs QDs are not strictly necessary to produce a rough GaAs surface. By proper tuning of the growth parameters (such as substrate temperature, growth rate and As pressure) during GaAs growth, stepped mounds may be obtained. Since such mounds are produced by the kinetics of growth, we preferred to use a buried InAs layer, yielding more reproducible results in terms of roughness.

The increased yield of QDMs on the surface enhances the probability to find QDMs during μ-PL investigations. For μ-PL studies, a low density InAs QDM sample, characterized by a surface density of 4×10^7 cm^{-2}, is grown on a surface with stepped mounds. A representative AFM image of an uncapped sample is shown in Fig. 4a.

Figure 4b shows an ensemble PL spectrum of the low density QDMs measured at 6 K. Three different peaks can be distinguished from the spectrum, i.e., the emission from the In(Ga)As wetting layer (WL), from the buried InAs QDs used to produce the stepped mounds and the emission from the QDMs. Due to the partial-capping and annealing method [15, 23] the QDM emission is blue-shifted and spectrally well separated from the emission of the underlying QD

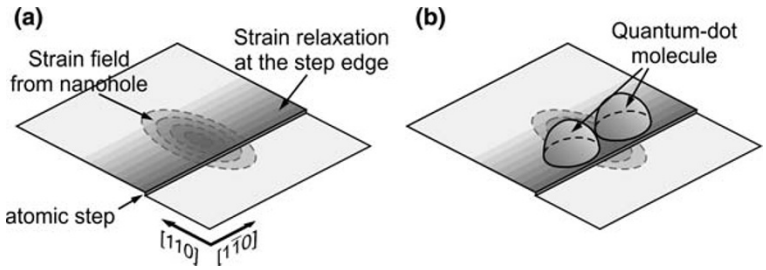

Fig. 3 Schematics of the surface strain configuration of filled nanoholes (**a**) and QDMs on the step edges (**b**). The gray scale corresponds to lower strain energy for In atoms

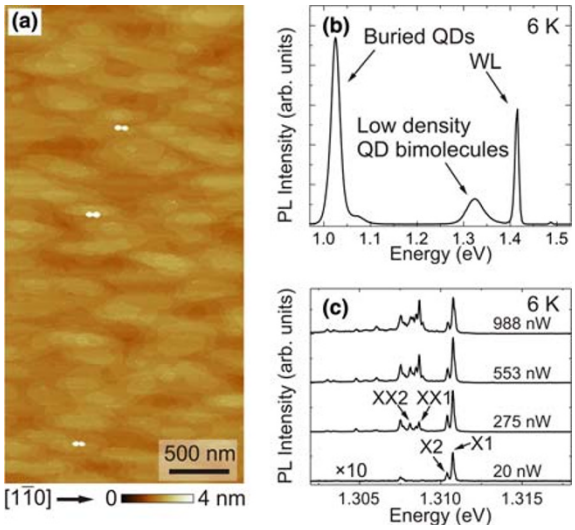

Fig. 4 AFM image (2×4 μm^2) of low density QDMs nucleated on stepped edge (**a**), photoluminescence (**b**) and μ-PL spectra of the QDMs at different excitation powers (**c**) recorded at 6 K

layer. The intensity difference between the QD and QDM peaks is attributed to the reduced density of the QDMs (see Fig. 4b) compared to the buried QDs.

Due to the extremely low density of QDMs, no shadow mask or patterning is required for single-molecule spectroscopy. Figure 4c shows μ-PL spectra of a representative single QDM at different excitation powers. At low excitation power, the spectrum is dominated by two resolution-limited sharp peaks labeled X1 and X2, whose intensities are linearly dependent on excitation power and saturate at high powers. These two peaks may be attributed to the recombination of excitons from the QDM, as suggested by detailed photoncorrelation experiments [24]. Besides these lines, two peaks labeled XX1 and XX2, appear at higher powers at the low-energy side of the excitonic emissions and may originate from the biexciton transitions. While the systematic study of the QDM optical properties is out of the scope of this work and has been presented elsewhere [24], we point out here that the spectra characterized by resolution-limited lines with no appreciable background underline the high structural quality of QD systems obtained by combining molecular beam epitaxy growth and in situ etching [16].

In summary, we have investigated the formation process of QDMs on a surface with stepped mounds. The yield of lateral QDMs is substantially increased with respect to growth on a flat surface [8]. The improved yield is attributed to the superposition of the strain field of the InGaAs filled-nanoholes and the strain relaxation at the step edges. The QDMs are Ga-richer compared to single QDs due to strain-enhanced intermixing. μ-PL spectra of a QDM sample characterized by high yield and low density witness the high optical quality of single QDMs.

Acknowledgment This work was financially supported by SFB/TR21 and BMBF (03N8711).

References

1. J.H. Reina, L. Quiroga, N.F. Johnson, Phys. Rev. A **62**, 012305 (2000)
2. G. Burkard, D. Loss, Phys. Rev. B **59**, 2070 (1999)
3. I. Shtrichman, C. Metzner, B.D. Gerardot, W.V. Schoenfeld, P. M. Petroff, Phys. Rev. B **65**, 081303 (2002)
4. H.J. Krenner, M. Sabathil, E.C. Clark, A. Kress, D. Schuh, M. Bichler, G. Abstreiter, J.J. Finley, Phys. Rev. Lett. **94**, 057402 (2005)
5. B.D. Gerardot, S. Strauf, M.J.A. de Dood, A.M. Bychkov, A. Badolato, K. Hennessy, E.L. Hu, D. Bouwmeester, P.M. Petroff, Phys. Rev. Lett. **95**, 137403 (2005)
6. E.A. Stinaff, M. Scheibner, A.S. Bracker, I.V. Ponomarev, V.L. Korenev, M.E. Ware, M.F. Doty, T.L. Reinecke, D. Gammon, Science **311**, 636 (2006)
7. T. Unold, K. Mueller, Ch. Lienau, T. Elsaesser, A.D. Wieck, Phys. Rev. Lett. **94**, 137404 (2005)
8. R. Songmuang, S. Kiravittaya, O.G. Schmidt, Appl. Phys. Lett. **82**, 2892 (2003)
9. T.v. Lippen, R. Nötzel, G.J. Hamhuis, J.H. Wolter, J. Appl. Phys. **97**, 044301 (2005)
10. O.G. Schmidt, Ch. Deneke, S. Kiravittaya, R. Songmuang, H. Heidemeyer, Y. Nakamura, R. Zapf-Gottwick, C. Müller, N.Y. Jin-Phillipp, IEEE J. Sel. Top. Quant. Electron. **8**, 1025 (2002)
11. S. Kiravittaya, R. Songmuang, N.Y. Jin-Phillipp, S. Panyakeow, O.G. Schmidt, J. Cryst. Growth **251**, 258 (2003)
12. B. Krause, T.H. Metzger, A. Rastelli, R. Songmuang, S. Kiravittaya, O.G. Schmidt, Phys. Rev. B **72**, 085339 (2005)
13. H. Schuler, T. Kaneko, M. Lipinski, K. Eberl, Semicond. Sci. Technol. **15**, 169 (2000)
14. A. Rastelli, S.M. Ulrich, E.-M. Pavelescu, T. Leinonen, M. Pessa, P. Michler, O.G. Schmidt, Superlatt. Microstruct. **36**, 181 (2004)
15. L. Wang, A. Rastelli, O.G. Schmidt, J. Appl. Phys. (in press)
16. A. Rastelli, S. Kiravittaya, L. Wang, C. Bauer, O.G. Schmidt, Physica E **32**, 29 (2006)
17. S.O. Cho, Zh.M. Wang, G.J. Salamo, Appl. Phys. Lett. **86**, 113106 (2005)
18. E. Placidi, F. Arciprete, V. Sessi, M. Fanfoni, F. Patella, A. Balzarotti, Appl. Phys. Lett. **86**, 241913 (2005)
19. B. Lita, R.S. Goldmana, J.D. Phillips, P.K. Bhattacharya, Appl. Phys. Lett. **75**, 2797 (1999)
20. O.G. Schmidt, K. Eberl, Phys. Rev. B **61**, 13721 (2000)
21. G. Biasiol, E. Kapon, Phys. Rev. Lett. **81**, 2962 (1998)
22. S. Kiravittaya, H. Heidemeyer, O.G. Schmidt, Appl. Phys. Lett. **86**, 263113 (2005)
23. J.M. Garcia, T. Mankad, P.O. Holtz, P.J. Wellman, P.M. Petroff, Appl. Phys. Lett. **72**, 3172 (1998)
24. G.J. Beirne, C. Hermannstädter, L. Wang, A. Rastelli, O.G. Schmidt, P. Michler, Phys. Rev. Lett. **96**, 137401 (2006)